

# The effect of angle restriction on the topological characteristics of minicircle networks

J. Arsuaga<sup>\*†</sup>, Y. Diao<sup>#</sup> and K. Hinson<sup>#</sup>

<sup>\*</sup>Department of Mathematics  
San Francisco State University  
1600 Holloway Ave  
San Francisco, CA 94132

<sup>#</sup>Department of Mathematics and Statistics  
University of North Carolina at Charlotte  
Charlotte, NC 28223

**Abstract.** Networks of topologically linked minicircle polymers are found in diverse natural systems and are a subject of intense research in nanotechnology. In a recent report the authors introduced a new theoretical model to study the effects of polymer density on the formation and on the topological properties of minicircle networks. Three key topological characteristics were identified in the formation and characterization of a network: the critical percolation density, the average saturation density and the mean valence of the network. In this work we report how these characteristics change when an orientation bias is imposed on the minicircles forming the network. We observe that such restrictions have significant effects on the key topological characteristics of the network. In particular while the effects of restriction of the tilting angle can be predicted we find that those of the azimuthal angle can have somewhat unexpected results.

AMS classification scheme numbers: 57M25 and 92B99.

## 1. Introduction

Networks of topologically linked minicircle polymers have been found in diverse biological systems such as those made of DNA and found in the kinetoplast of trypanosomes (reviewed in [?]) or those made of proteins and found in the protein capsid of bacteriophage HK97 [?]. Polymer networks have also been engineered. For instance olympic gels, used in the area of ferromagnetic nanoparticles [?], consist of a network obtained from a polymer melt made of short ring polymers and of very short linear polymers with reactive ends (i.e. the ends can join together to make a circular molecule). DNA engineered minicircle networks include Borromean rings of DNA [?], catenated scaffolds [?, ?] and those generated by type II topoisomerases [?].

A key parameter affecting the formation of topological links and of networks is the orientation of minicircles. The relative orientation of catenated minicircles is being investigated in nanotechnology to design molecular motors and switches (reviewed in [?, ?]). In trypanosomes minicircles are found roughly parallel to each other and perpendicular to the disk-plane of their containing structure (called kinetoplast disk)

† To whom correspondence should be addressed (jarsuaga@sfsu.edu)

[?]. It is thus our goal here to develop a theory of the topological changes that occur on network formation when minicircle orientation is taken into account.

A pioneer study on the topological properties of minicircle networks was done by de Gennes motivated by the design of olympic gels [?]. However a theory for network formation is still lacking. In an earlier report [?], and inspired by the problem of kinetoplast DNA [?], we introduced a model to analyze how the topological properties of a monolayer minicircle network change as a function of minicircle density. We call this model the Square Lattice Minicircle model, or SLM model for short. In this model randomly oriented minicircles of equal radius are placed on the vertices of the simple square lattice. *Minicircle density*, defined as the number of minicircles per unit area (and equals  $1/r^2$  where  $r$  is the distance between the centers of two adjacent minicircles in the SLM model), is varied and the topological properties of the resulting linked clusters calculated. We rigorously showed that a high density of non-repelling minicircles naturally leads to the formation of a network. Furthermore the SLM model predicts that the formation of a network by increasing density undergoes a critical phase, percolation phase, in which large clusters of linked minicircles become highly probable. Our model also predicts a linear relationship between valence and density, a phenomenon observed in the replication cycle of certain trypanosomes during which the mean valence of the network doubles from 3 to 6 as the number of minicircles doubles (from 5000 to 10000) [?]. The mathematical model proposed in this paper extends the SLM model proposed in [?] by characterizing the effects of minicircle orientation on the topological properties of the network. In particular we here characterize the effects of restricting the tilting and the azimuthal angles on the network formation. This problem is also motivated by the organization of minicircles in trypanosomes which are believed to be organized almost parallel to each other and perpendicular to the kinetoplast disk (reviewed in [?]).

It is important to point out that while the simplicity of the SLM model and the generalization presented here allowed us to carry out simulation and analytical studies, it is not a realistic model. Notably, the SLM model assumes that minicircles are rigid, have no thickness and their centers are confined to a lattice. Hence our numerical estimations of percolation and saturation densities should be used as a qualitative guidance for more realistic models.

## 2. Basic Definitions and Methods

### 2.1. The SLM model and its characteristics of interest

The SLM model considers a monolayer of randomly oriented flat minicircles which are centered at the vertices of a square lattice (*i.e.* a gridded square region in the  $xy$ -plane). In this setting we consider that two minicircles are *linked* if one cannot separate them without breaking them first. More generally, a set of minicircles form a *linked cluster* if one cannot separate them into two parts without breaking any of the minicircles. The linking between two minicircles can be computed easily and details can be found in [?]. Given a square grid of minicircles, a linked cluster of minicircles that contains minicircles on the opposite boundaries of the square grid is called a *percolating cluster*. The *critical percolation density*, or just *critical density*, is a positive value  $D_c$  with the following property: if the density  $D > D_c$ , then there exists a positive constant  $\alpha > 0$ , such that the probability for a minicircle grid to form

a network is at least  $\alpha$ , regardless what is the dimension of the grid. On the other hand, if  $D < D_c$ , then the probability of the the formation of a network goes to zero as the dimension of the grid goes to infinity. In this work we use this critical density to define a *minicircle network* and say that a grid of minicircles forms a *network* when a percolating cluster exists in the grid. In the case that we are not certain whether the minicircles on the given lattice grid has formed a network, we will call the system a *minicircle grid* instead. When most minicircles in a minicircle network fall into the same linked cluster, we say that the network *saturates*. Here 99% saturation level means that there exists a linked cluster in the minicircle network that contains at least 99% of the minicircles in the grid. In this study, a saturated minicircle network means a network with a 99% saturation level. For a given minicircle in the minicircle grid, its *valence* is defined as the number of minicircles that are linked to it directly. The mean *valence of a minicircle* is defined as the average valence of a minicircle over a set of different networks. The *average valence of a minicircle grid* (in which the minicircles are fixed) is the average of the valences of all minicircles in the grid. The average valence of a minicircle grid is not necessarily an integer. However, if the grid is of sufficient size, then its average valence can be well estimated by the mean valence of a minicircle in a minicircle grid of the same size.

## 2.2. Methods for angle restrictions and sample generation

The orientation of a minicircle (in a minicircle grid) is determined by its normal vector, which is in turn determined by two angles: the *tilting angle* and the *azimuthal angle*. The tilting angle (denoted by  $\theta$ ) is the angle between the normal vector and the positive  $z$ -axis, while the azimuthal angle (denoted by  $\phi$ ) is the angle between the projection of the normal vector to the  $xy$ -plane and the  $x$ -axis. In the unrestricted case [?], the normal vector of a minicircle is assumed to be uniformly distributed over the unit sphere. It follows that  $\theta$  is a continuous random variable taking values in  $[0, \pi]$  and  $\phi$  is a continuous random variable taking values in  $[0, 2\pi]$ . It is well known that  $\cos \theta$  is uniformly distributed in  $[-1, 1]$  while  $\phi$  is uniformly distributed in  $[0, 2\pi]$ .

Let  $\theta_0, \phi_0$  be two angles such that  $0 \leq \theta_0 \leq \pi/2$  and  $0 \leq \phi_0 \leq \pi/2$ . The angle restrictions implemented in this paper are of the form  $\theta \in [\theta_0, \pi - \theta_0]$  and  $\phi \in [\phi_0, \pi - \phi_0] \cup [\pi + \phi_0, 2\pi - \phi_0]$  for various values of  $\theta_0$  and  $\phi_0$ .  $\theta_0$  will be called the *tilting angle restriction* and  $\phi_0$  will be called *azimuthal angle restriction*. In the extreme case that  $\theta_0 = \pi/2$ , the minicircles would be perpendicular to the lattice plane. And if  $\phi_0 = \pi/2$ , then all minicircles would be parallel to each other. These correspond to the reported observations in trypanosomes minicircles [?]. We choose a wider and varied range of the parameters  $\theta$  and  $\phi$  in our study so that our results can be referred to in other angle restriction conditions when applicable. Of course, one may also consider angle restrictions of other forms. The point we will be making is that different angle restrictions may yield very different results. Under the angle restriction,  $\cos \theta$  is uniformly distributed in  $[-\cos \theta_0, \cos \theta_0]$  and  $\phi$  is uniformly distributed in  $[\phi_0, \pi - \phi_0] \cup [\pi + \phi_0, 2\pi - \phi_0]$ . These form the foundations of our minicircle generating algorithm. The left side of Figure ?? is a visual definition of the tilting angle and azimuthal angle of a minicircle with respect to the axes of the lattice. The right side is an illustration of a minicircle grid with tilt and azimuthal restrictions.

We generated minicircle grids of dimensions up to  $1000 \times 1000$ . Notice that larger

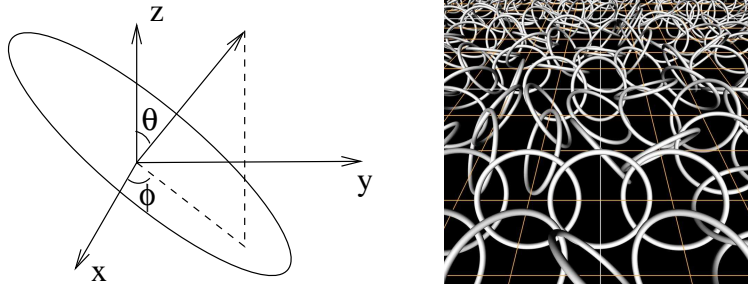


**Figure 1.** Left: The tilting angle  $\phi$  and azimuthal angle  $\theta$  of a minicircle with respect to the  $x$  and  $y$  axes of the lattice plane. Right: A network of minicircles in the simple square lattice with tilting and azimuthal angular restrictions.

scale grids were not necessary because the key characteristics such as the critical percolation density and the average saturation density are fairly robust measurements that can be fairly well estimated using these dimensions. For a fixed number of minicircles increasing the density is equivalent to increasing the radius of the minicircles simultaneously while keeping the size of the lattice edges fixed. We used this characterization in the implementation of our algorithms. During this process of density increasing, minicircles were allowed to freely perform strand passages. Ensembles of minicircle grids were obtained for each fixed radius  $r$ .

### 3. Numerical results

In this section, we present the numerical results in our investigations on the effects of restricting the tilting and the azimuthal angles on the critical percolation density, on the average saturation density, as well as on the growth rate of the mean valence. We also estimate the homogeneity of the network by analyzing the cumulative distribution of the mean valence.

#### 3.1. The case of the tilting angle restriction

Here we restricted the tilting of the minicircles while leaving the Azimuthal angle unconstrained. It was shown in [?] that given two randomly minicircles  $c_1$  and  $c_2$  of unit radius whose centers are fixed at a distance  $2r$  apart, the linking probability between  $c_1$  and  $c_2$  is  $1 - r$  for  $r \in [0, 1]$  and 0 for  $r > 1$ . The linking probability  $p_{r,\theta_0}$  between two minicircles with a tilting angle restriction  $\theta_0$  (where  $2r$  is the distance between the centers of the two minicircles) remains to be determined. Although an explicit formula for the general case  $\theta_0 \in (0, 90)$  is not yet derived, it is conceivable that  $0 \leq p_{r,\theta_0} \leq p_{r,0} = 1 - r$  (for  $0 \leq r \leq 1$ ). In the extreme case of a tilting angle restriction  $\theta_0 = \pi/2$ , the minicircles generated are in planes perpendicular to the  $xy$ -plane, hence no linking can occur between the minicircles, i.e.,  $p_{r,\pi/2} = 0$ . To estimate the linking probability for different angles we estimated  $p_{r,\theta_0}$  for  $r = 0$  to 1 with an increment of .05 and for  $\theta_0 = 0$  to 80 with increments of 10. Figure ?? shows the numerical estimations of  $p_{r,\theta_0}$  for various  $\theta_0$  values. As expected for each fixed  $r \in (0, 1)$ ,  $p_{r,\theta_0}$  is a strictly decreasing function of  $\theta_0 \in [0, 90]$  and  $\leq 1 - r$ .

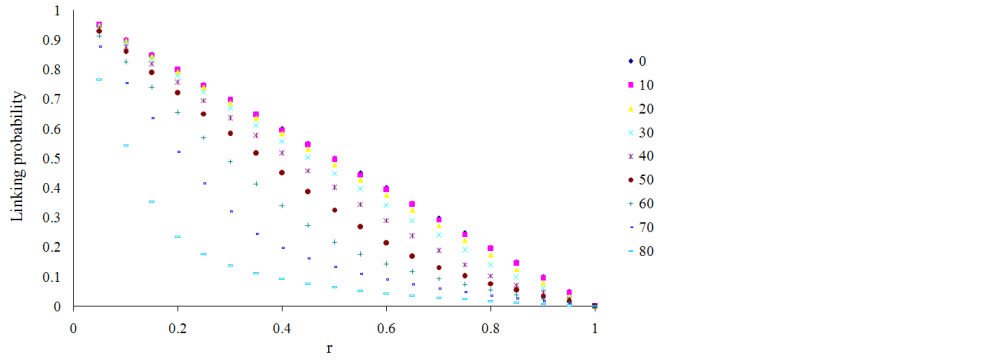


**Figure 2.** Numerical plots of the probability  $p_{r,\theta_0}$  for  $\theta_0 = 0$  to  $\theta_0 = 80$  degrees with an increment of 10 degrees as shown in the legend.

Next we characterized the three key topological characteristics, namely the critical density  $D_c$ , the average saturation (for 99% saturation)  $D_s$  and the mean valence of minicircle networks with tilting angle restriction. Figures ??, ?? and ?? summarize our calculations. In the case of critical percolation and saturation densities, tilting angle restrictions of 0 to 80 degrees with an increment of 10 degrees are used. Since  $p_{r,\theta_0}$  is a decreasing function of  $\theta_0$  for fixed  $r$  we would expect higher  $D_c$  and  $D_s$  values for larger  $\theta_0$  values. Results for  $D_c$  are shown in Figure ??. We observe an expected asymptotic behavior at  $x = 90$  and the data are fit by the function  $y = 0.3 + \frac{29.66}{90-x}$  (where  $y$  is the critical percolation density and  $x$  is the tilting angle restriction) has an  $R^2$  value of .996.

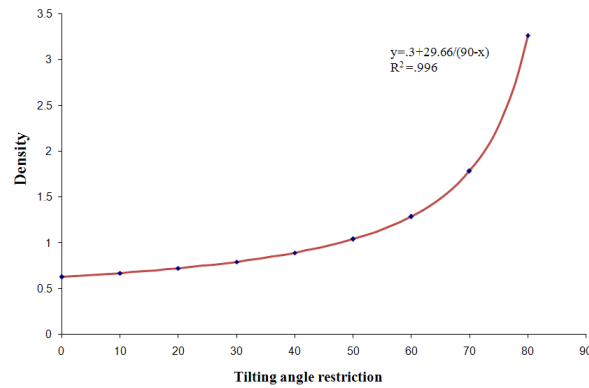


**Figure 3.** Estimated critical percolation density for various tilting angle restrictions. Each data point in the figures is based on samples of sample size 1000 and minicircle grids of dimension  $1000 \times 1000$ . The 95% standard error bars are less than .0006 in all cases except the case  $\theta_0 = 80$ , where the error bar is about .001.

A similar results holds for the saturation densities. Figure ?? shows the results. The function  $y = 0.8 + \frac{265.7}{(90-x)^{1.5}}$  (where  $y$  is the mean saturation density and  $x$  is the tilting angle restriction) fits the data well with an  $R^2$  value of .998 and captures the

asymptotic behavior at  $x = 90$ . By comparing the results from Figures ??, ?? one concludes that an increase in percolation density implies an increase in the saturation density.

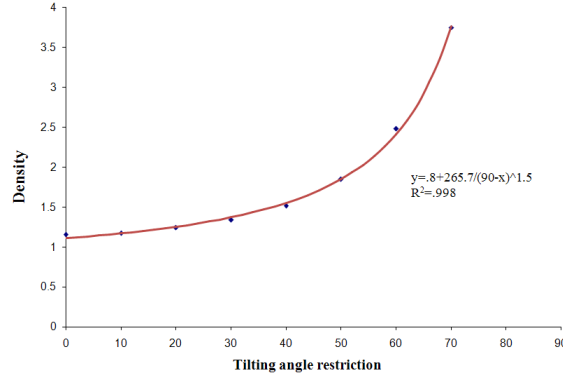


**Figure 4.** Estimated average saturation density for various restriction angles. Each data point in the figures is based on samples of sample size 1000 and minicircle grids of dimension  $1000 \times 1000$ . The 95% standard error bars are less than .0005 in all cases.

In the case of the mean valence, as discussed in [?], we are expecting a strong linear relationship between the mean valence and the minicircle density. That is, we expect that the growth of the mean valence to be of the form  $a(\theta_0) + b(\theta_0)D$ , where  $D$  is the density of the minicircle grid and  $b(\theta_0)$  is a decreasing function of the restriction angle  $\theta_0$  of the minicircles such that  $b(\theta_0) \rightarrow 0$  as  $\theta_0 \rightarrow 90$ . Again, this is because  $p_{r,\theta_0}$  is a decreasing function of  $\theta_0$  and  $p_{r,90} = 0$ . For comparison purposes, the results for restriction angles 0, 30, 60 and 87 are plotted together in Figure ??. The equations are given by  $y = 0.178x - 0.063$ ,  $y = 2.042x - 0.722$ ,  $y = 3.604x - 0.847$  and  $y = 4.173x - 0.871$  respectively. Notice the excellent fitting quality as indicated by the  $R^2$  values of the regression given by  $R^2$  and all  $\geq 0.998$ .

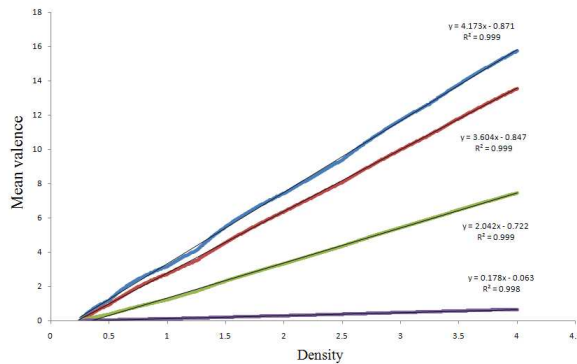


**Figure 5.** The mean valence as a function of the density under the tilting angle restrictions of 0, 30, 60 and 87 degrees.

An important aspect of the minicircle network is its homogeneity. A network is considered to be homogeneous if each minicircle in the network is linked to the same number of minicircles with few exceptions. In the case that the angles are not restricted, we found the minicircle networks to be not homogeneous [?]. It turns out that this is still the case when the restriction in the tilting angle is considered. For a given minicircle, we estimate the homogeneity of the network by estimating  $p_i$  the probability that the valence of the minicircle is  $\geq i$ . If most minicircles are linked to, say, 3 other minicircles, then the cumulative density functions of  $p_i$  would be very small or even diminish for  $i \geq 4$  for the density range considered, while the cumulative density function of  $p_i$  for  $i \leq 3$  would reach values close to one before the network saturates. Figures ?? and ?? show the estimated cumulative density functions of  $p_i$  for  $i = 1$  to 7 under the tilting angle restrictions  $\theta_0 = 30$  and  $\theta_0 = 60$ .

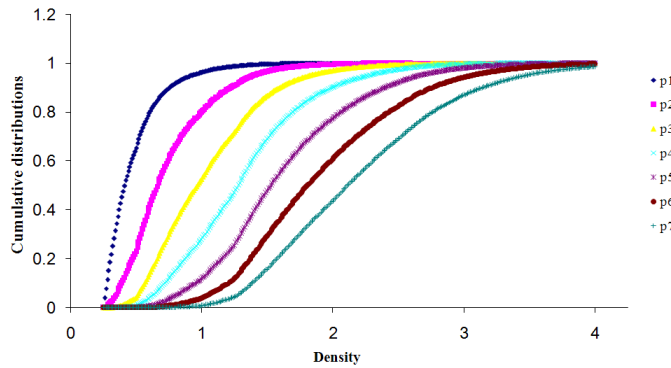


**Figure 6.** The cumulative distributions of  $p_1$  to  $p_7$  under the tilting angle restriction  $\theta_0 = 30$ .

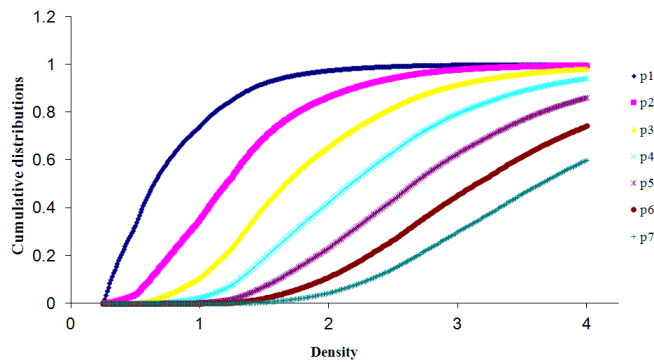


**Figure 7.** The cumulative distributions of  $p_1$  to  $p_7$  under the tilting angle restriction  $\theta_0 = 60$ .

As the density increases, each of these functions increases (even for the  $i$  values not shown in the figures), indicating that the minicircle grids are generally non-homogeneous. From these two figures one can again observe a strong dependency

of these cumulative distributions of  $p_i$  on the tilting angle restriction, namely that a larger restriction leads to a smaller cumulative density function value at a given density.

### 3.2. The case of the azimuthal angle restriction

Recall that a restriction of 0 degrees on the azimuthal angle means no restriction while a restriction of 90 degrees on the azimuthal angle means that all minicircles have normal vectors whose projections are parallel to the  $y$ -axis. The restrictions in the azimuthal angle present a case more complex than the tilting angle for the following reason: any two minicircles adjacent along the  $x$ -direction will link with probability 1 under the 90 degree restriction of the azimuthal angle, provided that the distance between the centers of the minicircles is less than 2. However, two adjacent minicircles along the  $y$ -direction will never link under this extreme restriction condition, and two adjacent minicircles along the diagonal lines parallel to  $y = x$  or  $y = -x$  will have positive linking probability only when the distance between their centers is less than 2. This fact has several implications when  $\phi_0 \approx 90$  that are discussed below. First, we investigated how the effects of the azimuthal angle restriction on the percolation density. Results are shown in Figure ???. The value for 0 restriction was already reported in [?]. When the restriction angle  $\phi_0$  is close to 90 degrees we expect a rather small critical percolation density (close to .25) since percolating clusters containing linked minicircles along the  $x$ -direction always form rapidly as the density passes over .25. A seemingly unexpected feature arose for other values of the restriction angle. As shown in Figure ??? the critical percolation density (as a function of the restricted azimuthal angle) is not a monotonically decreasing function. In fact, there is a local minimum near  $\phi_0 = 30$ . However, there is no reason why we should expect a monotonically decreasing curve either. In fact, the linking probability function  $p_{r,\phi_0}$  is no longer well defined, since two minicircles of the same distance may now have different linking probability depending on their relative positions in the plane. Hence a clear relation between the linking probability and the critical percolation density (as in the case of the tilting angle restriction) is lacking. To guide the trend of the data we fitted a polynomial of degree 6.

Next we studied the change of the average saturation density and results are shown in Figure ???. As in the case of the percolation density the value of the saturation density for  $\phi_0 = 0$  had been previously estimated [?]. Since minicircles adjacent along the  $y$ -direction do not link until the grid step becomes less than  $\sqrt{2}$  (which corresponds to a density of  $1/2$ ), the average saturation density has to be larger than .5. In fact, for  $\phi_0 = 90$  degrees,  $D_s$  is estimated to be around .56. A trend similar to that observed for the percolation density is also observed here. One important observation based on Figures ??? and ??? is that the  $\phi_0$  value that corresponds to the maximum critical percolation density does not produce the largest average saturation density. This shows that in general when comparing two minicircle grids, the minicircle grid with the smaller critical percolation density may have a larger average saturation density.

The mean valence also showed results different to those reported for the tilting angle. In the case of unrestricted angles, the contribution of a minicircle around the given minicircle to this slope are symmetric under rotations. This is still the case when we impose tilting angle restriction. However, for the azimuthal angle restrictions we impose, this symmetry is broken. In other words even if two minicircles are at the

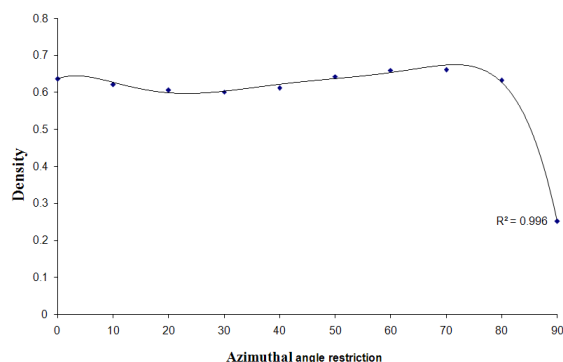


**Figure 8.** The estimated critical percolation densities at different restriction angles. The data are obtained on minicircle grids of dimension  $1000 \times 1000$  with sample size of 1000. The left end of the graph represents the unconstrained case previously reported. The 95% standard error bars are less than .00025 in all cases.

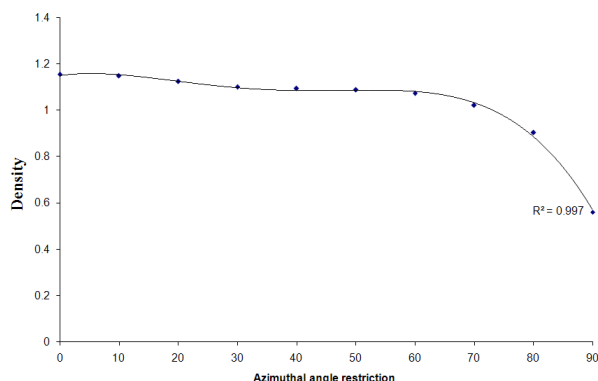


**Figure 9.** The average saturation density estimated at different restriction angles. The data are obtained on minicircle grids of dimension  $1000 \times 1000$  with sample size of 1000. The 95% standard error bars are less than .0003 in all cases and the fitting function is a polynomial of degree 4.

same distance from a given minicircle they may not have the same contribution in the computation of the mean valence of the given minicircle. Thus the mean valence of a given minicircle may not have a strong linear relation with the density. This breaking of the linear relation is demonstrated in Figure ?? using  $\phi_0 = 87$  degrees. One way to comprehend the result shown in Figure ?? is to compare it with the extreme case where  $\phi_0 = 90$  degrees (since  $\phi_0 = 87$  degrees is very close to 90 degrees). In this case the line that is parallel to the  $x$ -axis and goes through the center of a minicircle will intersect the minicircle in a diameter. Thus linking can only become possible between minicircle adjacent to each other along the  $x$  direction. In fact, the linking probability between any two such minicircles is 1 when the distance between the centers of the two circles (along the  $x$  direction) is less than 2. Recall that the density is equal to  $1/r^2$  where  $r$  is the distance between the centers of two adjacent minicircles. Thus, the

valence of each minicircle (in the extreme condition that  $\phi_0 = 90$  degrees) is exactly 2 if  $1 < r < 2$  (since each minicircle will link with its two immediate neighbors along the  $x$  direction with probability one), is exactly 4 if  $2/3 < r < 1$  (since each minicircle will link with its four closest neighbors along the  $x$  direction with probability one), is exactly 6 if  $1/2 < r < 2/3$ , and so on. Translating this into the densities, one would expect a horizontal step function that takes value 2 for  $.25 < D < 1$ , 4 for  $1 < D < 9/4$ , 6 for  $9/4 < D < 4$ , and so on. Figure ?? is really a distortion of this step function due to the fact that with  $\phi_0 = 87$  degrees, minicircles neighboring each other along the  $x$  direction do not link with probability one even if their centers are close (but this linking probability is indeed an increasing function of the distance between their centers) and that other minicircle pairs may also link.

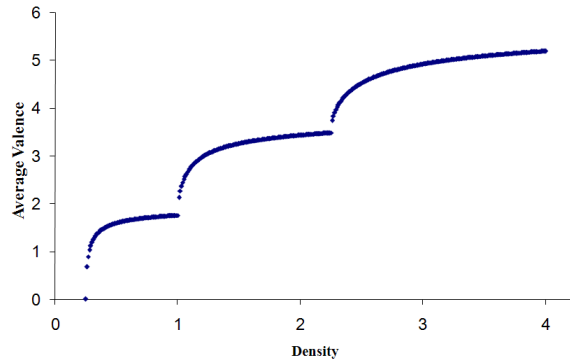


**Figure 10.** The estimated mean valence when the azimuthal angle is restricted to  $\phi \geq 87$ .

We concluded this study by determining the homogeneity of the networks by means of the cumulative distribution. In the case of the azimuthal angle restriction, the cumulative probability density function is less smooth due to the fact that linking probability between minicircles of the same distance varies depending on the relative positions of the minicircles involved. This phenomenon is more profound when the angle restriction  $\phi_0$  is large, as shown in Figure ??.

#### 4. Discussion and ending remarks

Networks of topologically linked circular synthetic polymers, DNA or proteins have been observed in nature or generated for nanotechnology purposes. How these networks grow as a function of minicircle density remains to be understood. In [?], and inspired by the linking of DNA minicircles in the kinetoplast of trypanosomes, we introduced the SLM model. Using this model we characterized the growth and the topological properties of a monolayer network of minicircles as a function of density. We analytically showed the existence of a critical percolation density  $D_c < 1$  and numerically estimated that  $D_c \approx 0.637$ . For a given minicircle grid of fixed dimension  $d \times d$ , the probability that the network saturates approaches one exponentially fast (so the average saturation density  $D_s$  must be finite) and our estimation of  $D_s$  in the limit case is  $D_s = 1.154$ . A linear relationship between the mean valence and the density

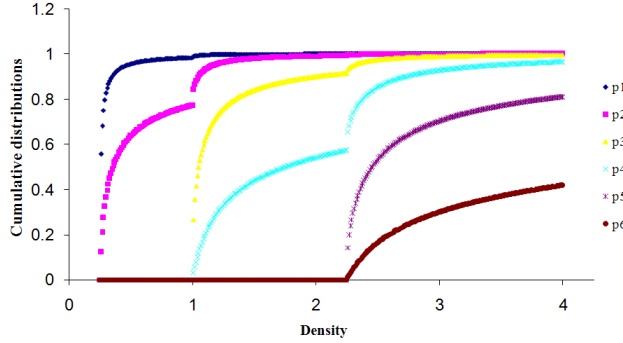


**Figure 11.** The cumulative distributions of  $p_1$  to  $p_6$  under the azimuthal angle restriction  $\phi_0 = 87$ .

was also derived. In that case the slope in the linear relation is the sum of the linking probabilities between any given minicircle and all other minicircles.

The SLM model assumes that minicircles are randomly oriented however experimental observation of biological systems and new nanotechnological devices suggest that the angle between minicircles is an important variable to consider. In this paper we studied the effects of minicircle orientation by characterizing the effects of constraining the tilting and the azimuthal angle. In each case the restriction is placed on one angle, while keeping the other angle un-constrained. We observed that both angle restrictions have significant impacts on the key topological characteristics (specially in the extreme cases) and that are difficult to derive analytically. For instance when estimating the percolation density one can consider the following example. At the grid step length  $2r = 3/(1 + \sqrt{2})$ , the sum of the linking probability between two adjacent minicircles along the  $x$  (or  $y$ ) direction and two adjacent minicircles along the diagonal  $y = x$  direction is  $1/2$ . And this grid step length corresponds to a minicircle density of  $1/(2r)^2 \approx .648$ . One would wonder whether this can be generalized to the case of tilting angle restriction. In other words, if  $r$  is a value such that  $p_{r,\theta_0} + p_{\sqrt{2}r,\theta_0} \approx .5$ , then  $D_c$  can be approximated by  $1/(2r)^2$ . Let us look at two examples here. Let's consider first the case  $\theta_0 = 50$ . In this case, we have  $p_{.45,50} \approx .38$  and  $p_{.45\sqrt{2},50} > p_{.65\sqrt{2},50} \approx .16$ , so  $p_{.45,50} + p_{.45\sqrt{2},50} > 1/2$ . On the other hand,  $p_{.5,50} \approx .33$  and  $p_{.5\sqrt{2},50} < p_{.7\sqrt{2},50} \approx .13$ , so  $p_{.5,50} + p_{.5\sqrt{2},50} < 1/2$ . Thus we would estimate  $D_c$  to be somewhere between  $1/(2 \cdot .5)^2 = 1$  and  $1/(2 \cdot .45)^2 \approx 1.23$ . The actual numerical value obtained is  $D_c \approx 1.067$ . Thus this rough estimation is still not too bad. However, things become much worse as  $\theta_0$  increases further. For example, at  $\theta_0 = 70$ ,  $p_{.3,70} + p_{.3\sqrt{2},70}$  is fairly close to  $1/2$ . But  $1/(2 \cdot .3)^2 \approx 2.78$  while our numerical estimation of  $D_c$  is around 1.88.

In the case of the tilting angle restriction, the relationship between the tilting angle restriction  $\theta_0$  and its impact on the critical percolation density and the saturation density is rather simple. This relationship is less straight forward in the case of the azimuthal angle restriction. It is conceivable that if one combines the two restrictions, then the situation will be more complicated. We conducted some special case studies to explore this. For example, with  $\theta_0 = 87$  and  $\phi_0 = 0$ , there is no network formation at density 4. However, with  $\theta_0 = 87$  and  $\phi_0 = 84$ , networks formed at densities less

than 4. At  $\phi_0 = 89$ , the critical percolation density is estimated to be just slightly over 1. However in this case we observed some kind of “resistance” to reaching percolation at any density less than 1, since not a single trial reached percolation at density less than 1. These findings are illustrated in Figure ??.

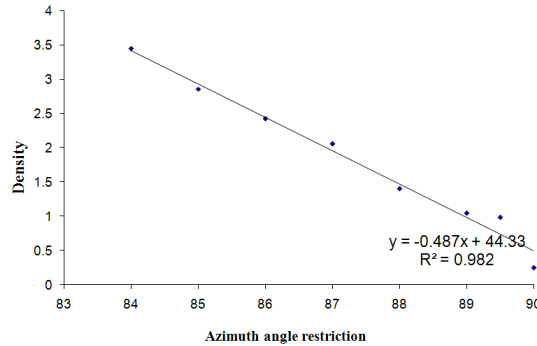


**Figure 12.** The estimated critical percolation densities under various azimuthal angle restrictions with the fixed tilting angle restriction  $\theta_0 = 87$ .

To summarize, our results show that the critical percolation density and the average saturation density, as well as the structure of the linking clusters, are quite sensitive to the angle restriction conditions. Furthermore while restrictions in the tilting angle have a somewhat predictable behavior, the growth of a network with restrictions on the azimuthal angles are somewhat less intuitive. In fact, in some extreme restriction conditions, the minicircles cannot even form links. For example when minicircles are completely parallel to each other or completely perpendicular to the lattice plane no clusters can form. This indicates that when studying systems of minicircles on grids a careful and detailed analysis of the angle restriction is necessary. Our work has provided some basic theoretical benchmarks in this regard. A potential application of our results is in the study of network formation in trypanosomes. In [?] a model for minicircle organization was derived based on the assumption that minicircles are randomly oriented. However it has been observed that minicircles are parallel to each other and perpendicular to the the kinetoplast disk. It is therefore natural to ask how the observed angle restriction affects the initial model of minicircle organization.

We end this paper with an outlook into the future study of this subject. The angle restriction is not the only factor that affects the percolation and saturation of a minicircle grid. For example, the choice of the lattice can also affect these critical densities, although in a less sensitive manner. This is the subject of study in another paper under submission [?]. As we pointed out earlier, the simplicity of the SLM model allowed us to carry out simulation and analytical studies and we believe that more sophisticated models will present similar behaviors to those discussed here. However, more realistic models can be developed for specific physical and biological systems. More realistic DNA models could for instance incorporate the flexibility and thickness of minicircles as well as variations on the positions of minicircles in space. Many obstacles will arise in developing and analyzing such models, it is our belief that these obstacles will be overcome and new information from the physical system will be

obtained from the theories developed.

**Acknowledgement** Support for this work came from NSF grants DMS-0920887 (J. Arsuaga), DMS-0920880 (Y. Diao and K. Hinson), DMS-1016460 (Y. Diao) and NIH grant 2S06GM52588-12 (J. Arsuaga).

## 5. References

- [1] Arsuaga J, Diao Y and Hinson K, submitted to *J. Phys A.: Math Gen.*
- [2] Balzani V, Credi A, Silvi S and Venturi M, *Chem Soc Rev*, **2006**, **35**(11), 1135–1149.
- [3] Chen J, Rauch C A, White J H, Englund P T and Cozzarelli N R, *Cell*, **1995**, **80**(1), 61–69.
- [4] Chen J, Englund P T and Cozzarelli N R, *EMBO J*, **1995**, **14**(24), 6339–6347.
- [5] Diao Y, Hinson K, Vazquez M and Arsuaga J, *J Mathematical Biology*, in press.
- [6] Diao Y and Janse van Rensburg E J, *Topology and Geometry in Polymer Science* (eds Whittington S G et al), **1998**, IMA Volumes in Mathematics and its Applications **103**, 79–88.
- [7] Diao Y, *J Knot Theory Ramifications*, **1984**, **3**(3), 379–389.
- [8] Duda R L, *Cell* **1998**, **94**(1), 55–60.
- [9] Kreuzer K N and Cozzarelli N R, *Cell*, **1980**, **20**(1), 245–254.
- [10] Liu B et al, *Trends Parasitol*, **2005**, **21**(8), 363–369.
- [11] Mao C, Sun W and Seeman N C, *Nature*, **1997**, **386**, 137–138.
- [12] Mayrhofer P, Schlee M and Jechlinger W, *Methods Mol Biol*, **2009**, **542**, 87–104.
- [13] Müller-Nedebock K K and Edwards S F, *J Phys A Math Gen*, **1998**, **32**, 3283–3300.
- [14] Raphaël E, Gay C and de Gennes P G, *J Stat Phys*, **1997**, **89**, 111–118.
- [15] Shafi KVPM et al, *J Phys Chem B*, **1999**, **103**, 3358–3360.
- [16] Shapiro T A, Englund P T, *Annu Rev Microbiol.*, **1995**, **49** 117–143.
- [17] Schmidt T L and Heckel A, *Nano lett*, **2011**, **11**, 1739–1742.
- [18] Simpson L, Sbicego S and Aphasizhev R, *RNA*, **2003**, **9**, 265–276.
- [19] Weizmann Y et al, *PNAS*, **2008**, **105**, 5289.
- [20] Wilner O I et al, *Nat Biotechnol*, **2009**, **4**, 249–254.

”for Table of Contents use only”

**The effect of angle restriction on the formation of minicircle networks:  
applications to kinetoplast DNA from trypanosomes**

J. Arsuaga, Y. Diao and K. Hinson

